ORIGINAL

http://dx.doi.org/10.22480/rev.unifa.v32n2.435.ing

Post-burn microscopic analysis of the material of the insert of the solid propellant rocket engine nozzle: results (Part II)

Análisis microscópico posterior a la combustión del material del inserto de la boquilla de un motor cohete en un propulsor sólido: resultados (Parte II)

Análise microscópica pós-queima do material do inserto da tubeira de motor foguete a propelente sólido: resultados (Parte II)

Ronald Izidoro Reis [I]
Wilson Kiyoshi Shimote [II]
Christian Frederico de Avila Von Dollinger [III]
Luiz Cláudio Pardini [IV]

ABSTRACT

In part I of this work the procedure of preparation of samples and important concepts were presented, such as ablation in the motor tubing and also that of ablative and re-radiative thermal protections. In part II, (presented in the this study), the characterization by stereo microscopy, optical microscopy and scanning electron microscopy (SNAM) of the CRFC composite used as an insert in the tubing of the S43 engine was performed in the post-burning condition. The analysis by optical microscopy, performed in the region around the throat section, showed that the erosion of the sample was more pronounced on the surface than that observed in the regions farther from the passage of the gas flow. The scanning electron microscopy, performed in the region around the throat section, provided a more in-depth analysis of the morphology of the composite material, allowing to identify details of the reinforcing rods, such as carbon fiber filaments and, in the pyrolytic carbon matrix, the different lamellae deposited by CVD.

Keywords: Solid propulsion. Composite material. Tubing Insert. CRFC Insert.

RESUMEN

La parte I de este trabajo presentó el procedimiento para la preparación de muestras y conceptos importantes, como la ablación en la boquilla del motor y también las protecciones térmicas ablativas y reirradiactivas. En la parte II, (presentada en el presente trabajo), se realizó, en la condición posterior a la combustión, la caracterización por estéreo microscopia, microscopia óptica y microscopia electrónica de barrido (MEV) del compuesto CRFC usado como un inserto en la boquilla del motor S43. El análisis de microscopía óptica, realizado en la región alrededor de la sección de la garganta, mostró que la erosión de la muestra era más pronunciada en la superficie que la observada en las regiones más alejadas del paso del flujo de gas. La microscopía electrónica de barrido, realizada en la región alrededor de la sección de la garganta, proporcionó un análisis más profundo de la morfología del material compuesto, permitiendo la identificación de detalles de las barras de refuerzo, como los filamentos de fibra de carbono y, en la matriz de carbono pirolítico, las diferentes láminas depositadas por CVD.

***Palabras clave*:** *Propulsión sólida. Material compuesto. Inserción de la boquilla. Inserto de CRFC.*

I. Institute of Aeronautics and Space – (IAE) – São José dos Campos/SP – Brazil. Doctor Degree in Metallurgical and Mining Engineering by Universidade Federal de Minas Gerais. E-mail: ronaldrir@fab.mil.br

II. Institute of Aeronautics and Space – (IAE) – São José dos Campos/SP – Brazil. Doctor Degree in Thermal Sciences by École Nationale Supérieure de Mécanique et d'Aérotechnique - ENSMA France. E-mail: wilsonwks@fab.mil.br

III. Institute of Aeronautics and Space – (IAE) – São José dos Campos/SP – Brazil. Doctor Degree in Science and Engineering of Materials by Universidade Federal de São Carlos. E-mail: christiancfavd@fab.mil.br

IV. Institute of Aeronautics and Space – (IAE) – São José dos Campos/SP – Brazil. Doctor Degree in Science and Engineering of Materials - University of Bath – Unite Kingdom. E-mail: pardinilcp@fab.mil.br

Received: 02/28/19 Accepted: 06/19/19

The acronyms and abbreviations contained in this article correspond to the ones used in the original article in Portuguese.

RESUMO

Na parte I deste trabalho foram apresentados o procedimento de preparação das amostras e conceituações importantes, como a ablação na tubeira do motor e também a de proteções térmicas ablativas e reirradiativas. Na parte II, (apresentada no presente trabalho), foi realizada, na condição pós-queima, a caracterização por estéreo microscopia, microscopia óptica e microscopia eletrônica de varredura (MEV) do compósito CRFC usado como inserto na tubeira do motor S43. A análise por microscopia óptica, realizada na região em torno da seção da garganta, mostrou que a erosão da amostra foi mais acentuada na superfície do que aquela observada nas regiões mais afastadas da passagem do fluxo de gases. A microscopia eletrônica de varredura, realizada na região em torno da seção da garganta, proporcionou uma análise mais aprofundada da morfologia do material compósito, permitindo identificar detalhes das varetas de reforço, como, por exemplo, os filamentos de fibras de carbono e, na matriz de carbono pirolítico, as diferentes lamelas depositadas por CVD.

Palavras-chave: *Propulsão sólida. Material compósito. Inserto de tubeira. Inserto de CRFC.*

1 INTRODUCTION

The thermal protections material are components of space vehicles that have the function of protecting external structures, metallic or composite material, from thermomechanical requests and thermal flows during all stages of flight. These thermomechanical requests and thermal flows can come from both external aerothermodynamic phenomena and internal flow to the rocket engine. The state-of-the-art Thermal Protection System (TPS) for aerospace applications is based on intrinsic ablative materials and re-radiating ablative materials. For the **TPS** that use intrinsic ablative materials, thermal energy dissipation occurs due to mass loss and material phase change. These materials shall present: resistance to high temperatures, resistance to erosion, thermal shock and impact, in addition to low thermal conductivity and specific high heat (SILVA, 2009). According to Gonçalves (2008) and Silva (2011), in the **TPS** that use re-radiative ablative materials, the dissipation of energy occurs through the return to the environment in the form of radiation of part of the energy absorbed from the external flow, and the remainder is conducted to internal regions of the material (a mechanism relatively simpler than that of intrinsic ablative materials). In addition, these re-irradiative materials have great emissivity (e > 0.8) and low erosion rate under extreme incident flow conditions, allowing to protect structures for a long period. In this class of materials can be listed the family of composites with a hybrid matrix of carbon/silicon carbide (C/SiC) and silicon carbide fiber composites and silicon carbide matrix (SiC/SiC).

Examples of use of TPS in external applications are attack edges, re-entry warheads, and fuel tank envelopes located externally to space vehicles. The internal applications of TPS correspond to tubing inserts of the rocket engine (LEE, 1993; I READ IT. HUANG; XU, 2017; RICCIO et al. , 2017; SUTTON, 2006).

According to Ribeiro, Gregori and Pardini (2008) the rocket engine tubing insert, typically represented by a Laval nozzle, is an important component of a propellant system of launching vehicles. In this subsystem, the gases resulting from the burning of the propellant reach high temperatures (@ 2900°C) and are expanded in the tubing, by the effect of striction in this region, which has the function of increasing the ejection speed (2500 m/s), aiming to obtain the desired thrust. By the end of the 1950s, rocket engine inserts were manufactured in graphite and presented limitations in dimensions and uniformity, that is, the processes of obtaining graphite no longer met the geometries and properties necessary for applications in larger rocket engines. On this occasion arise the carbon composites reinforced with carbon fibers (CRFC), formed by carbon matrix and carbon fibers, which have added significant advances in the technology of preforms (multidirectional reinforcement architecture) for composites. The use of these preforms allowed the limitation of dimensions and geometry to be supplanted. In addition, the use of carbon fibers guaranteed the mechanical strength and tenacity necessary to ensure the satisfactory performance of the component. Pardini, Gonçalves and Vieira (2002, p. 2163) cite that

> [...] The number of directions of the preform is directly linked to the isotropy of the composite material to be obtained, that is, the greater the number of directions the closer to isotropy the material will be.

As isotropy is directly linked to the increase of fiber directions in the reinforcement architecture, it is usual to use unidirectional composites in the form of pins or rods that allow the arrangement of reinforcement in multiple directions. The obtainment of these pins or rods is performed by the pultrusion molding method, as illustrated in Figure 1.

Figure 1 – Sample of the pultrusion process for obtaining profiles and beams of various geometries with the use of one-way reinforcing fibers.

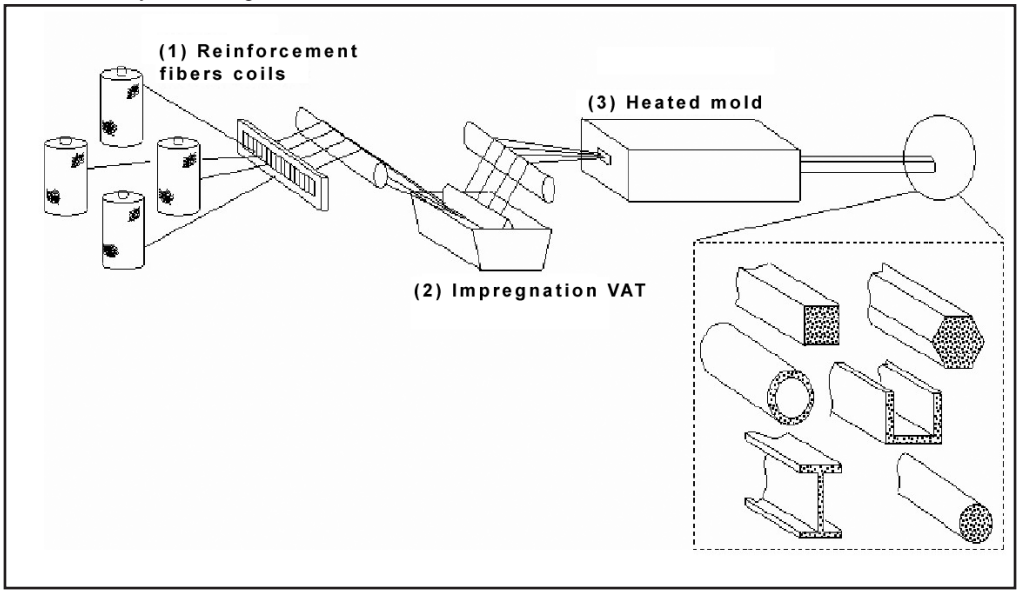

Source: Levy Neto and Pardini (2016, p. 202).

In this process, the reinforcing cables in the form of continuous fiber wicks are impregnated in a vat, where the resin, previously formulated and with adequate viscosity, allows impregnation. The most important process parameter in this case is the adequacy of the gel time of the resin, which must be tightly controlled, avoiding its premature curing when entering the heated mold. After impregnation, the fiber/polymer matrix assembly enters the mold, which will give a geometry to the component you want to obtain (LEVY NETO; PARDINI, 2016).

The pultrusion process allows to continuously obtain composite parts with defined cross-section geometry, such as circular and hexagonal shapes. In this way it is possible to obtain pins or slender sticks of small diameter pre-stiffened.

Ribeiro (2006, p. 33) cites that "[...] the diameter range suitable for preform use is between 0.5 - 3.0 mm". These rods (pins) are corresponding to unidirectional composites and, in pultrusion molding processes, they have fractions in volume of fibers equivalent to 65-70%.

With the obtaining of pins or rods it is possible to mount preform with multidirectional fiber architecture. According to Levy Neto and Pardini (2016, p. 155), both structures with severe thermo-structural requirements and those requiring greater property isotropy can be manufactured with this technology. In this class, the orthogonal (3D) tri-directional preforms are grouped, as shown in Figure 2(a), tetra-directional preforms (4D), in the plane and pyramidal, presented respectively in Figures 2(b) and (c), and can reach up to 11 distinct directions (11D). There are modern processes to obtain these structures but that, nevertheless, involve high cost due to investment in automated equipment.

Figura 2 – Preforms: (a) tri-directional (3D), tetra-directional (4D); (b) orthogonal [Z, 60º,0º]; and (c) vertex-diagonal (pyramidal).

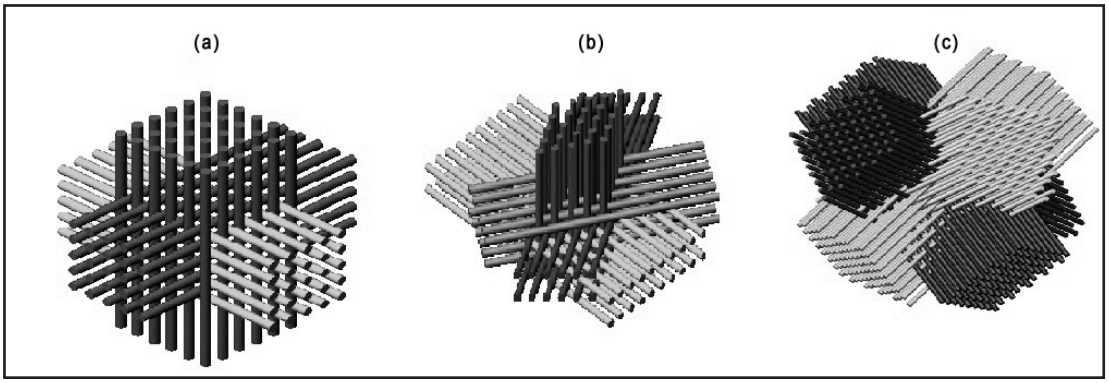

Source: Levy Neto and Pardini (2016, (a) p.156; (b) and (c) p.157).

The variation in the wear of the insert material along the output axis of the gas flow occurs due to differences in the temperature and velocity characteristics of the flow gases, as can be seen in the graphs in Figure 3.

Figure 3 – Temperature and speed profile of gases along the insert material.

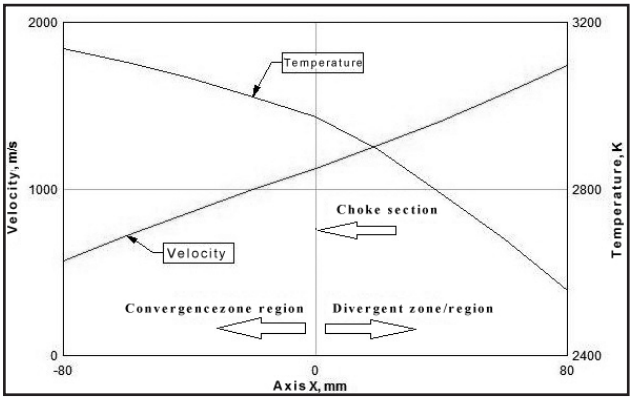

Source: The author.

Figure 3 shows the gases temperature and velocity profiles in the convergent and divergent regions of the tubing insert. It is observed in the figure that both in the convergent and divergent regions there is an increase in speed along the length of the insert from high temperatures (~3000K) to temperatures close to the environment. Between the convergent and divergent regions there is the throat section, where the combination of high pressure, high temperature and high flow speed on the surface of the material lead, as a result, to greater ablative and erosive effects.

2 METHODOLOGY

The evaluation of the internal surface of the insert after the passage of the hot gas flow from the burning of the S43 engine propellant was performed essentially by visual inspection, stereomicroscopy, optical microscopy, and scanning electron microscopy (SEM) techniques. These analyses are fundamental to assess the correlation of the test conditions and the behavior of the material, for this purpose, the section of determined regions of the component/insert is initially made. The main effect in the region of the throat of the tubing, resulting from the passage of hot gases from the burning of the propellant, is abrasion wear, causing removal on the surface and burning of the material. To systematize the analysis, a sample of the insert of the tubing of the S43 engine was taken, as shown in Figure 4(a). Figure 4(b) shows the subdivision of the sample into three regions for further microscopic evaluation. However, conceptually, there are only two regions, which are the convergent and divergent regions, as shown in Figure 3. In addition, there is the section of the throat that, besides delimiting these regions, characterizes the transition between subsonic (M<1) and supersonic (M>1) flow. Near this section it is expected a more significant erosion due to the conjunction of the thermal and mechanical effects of the flow.

Figure 4(b1) visually shows, in perspective, the subdivision of the sample into three regions as previously mentioned: divergent **D**, Throat **T**, and convergent **C**. Moreover, as shown in Figure 4(b2), the upper face of the three regions of the sample was divided into quadrants.

Figure 4 – Insert and sample of the S43 engine tubing. (a) Sample and Insert; and (b) Sample: (b1) Perspective image and (b2) top view.

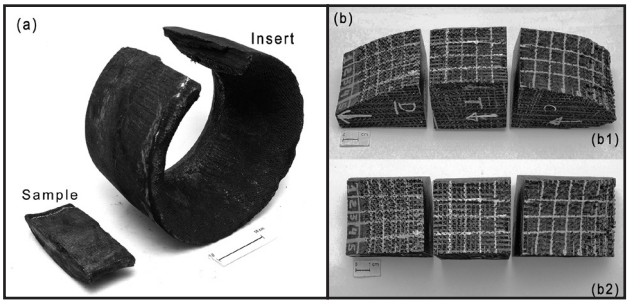

Source: The author.

The quadrants are characterized by rectangular units of approximately 1 cm^2, where it was agreed to call cij as being i the i-th quadrant along the cross-section of the convergent sample and e j the j-the column along the longitudinal section of the convergent sample, that is, along the length. Therefore, in Figure 5(a), c11 refers to the first row and first column of the sample, c21 refers to the second row and first column of the sample. The same criterion was adopted for the throat samples, Figure 5(b) and divergent, Figure 5(c).

Specifically, for the throat sample **T**, in addition to stereomicroscopy, microstructural analyses were performed by optical microscopy, both in regions close to and far from the passage of gas flow, from the burning of the propellant and, finally, surface analysis by SEM. For the study by optical microscopy, a region perpendicular to quadrant T 34 was determined. In this, the inlay, sanding and polishing was done to later record the images in the places near and away from the flow of gases from the burning of the propellant.

Figure 5 – Stratification image and identification of sample regions. (a) Convergent **C** (b) Throat **T**, and (c) Divergent **D**.

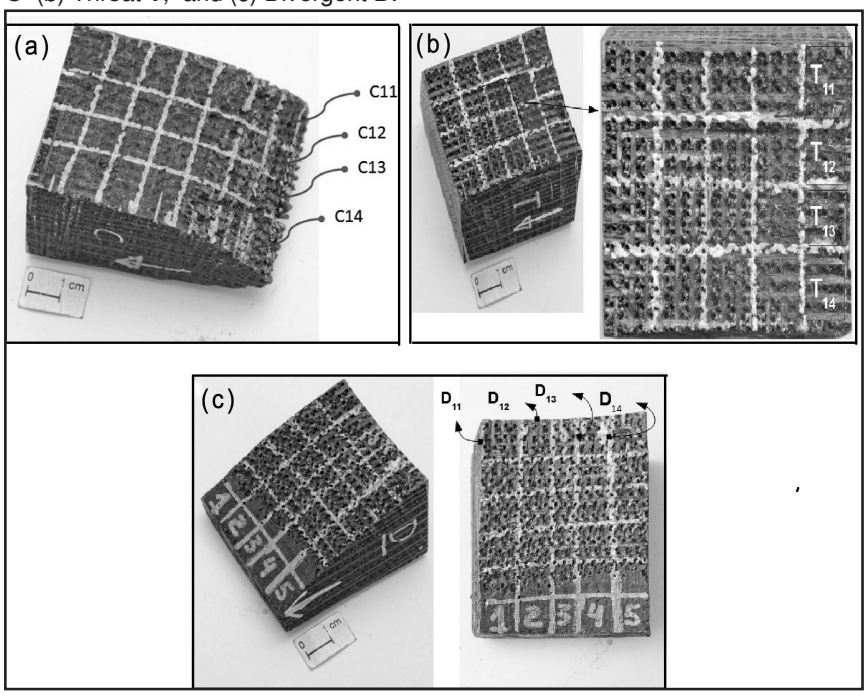

Source: The author.

2.1 Stereomicroscope

The three regions of the sample, divergent **D**, throat **T**, and convergent **C**, were examined in a Zeiss stereo microscope, Discovery V8 model, with coupled ICc1 digital camera (1,3 MP) and image capture system composed of microcomputer and Software *Axiovision* v 4.8. For lighting it was used the VISILED © system composed of LED lighting ring and control module, allowing for the alternate lighting of the LEDs and adjustment of the light intensity.

2.2 Optical microscopy

The throat sample was examined under an optical microscope Carl Zeiss, model *AxioImager* A2m, by reflected light technique using coupled ICc3 digital camera (3MP) and image capture system installed in the Materialography Testing Laboratory (LMAT/AMR/IAE).

The preparation of the specimens, for examination by optical microscopy, was performed following the operational procedures of the LMAT according to the requirements of the ASTM E3 (AMERICAN SOCIETY FOR TESTING AND MATERIALS, 2017). In this preparation, the specimens were sectioned with a disc of diamond cutting, in a metallographic cutter of BUHELERISOMET 1000 precision, with 50 gf load and 300 rpm rotation without cooling.

After sectioning, the samples were embedded in polyester resin. The preparation procedure of the observation surface under the microscope consisted of sanding in water sandpaper with abrasive SiC, with granulometry of 600 and 1200 mesh. Between each sanding stage, the specimens were rotated at 90°. After sanding, the specimens were polished in synthetic wool felt and diamond abrasive paste with granulometry of 3 μm and 1 μm. The final finishing polishing was performed in wool felt and colloidal silica with granulometry 0.06 μm.

2.3 SEM Analyses

For the SEM analysis, the electron microscope SEM LEO 435VPi and secondary electron detector (SE) were used, with 15 kV voltage application with the support of the INCA software of the subdivision of tests (AMR-E). The equipment is installed in the Scanning Electron Microscopy Testing Laboratory (SEML/AMR/IAE).

The use of SEM is a complementary analysis technique of great importance for the identification of the wear mechanism, by observing the surface of the insert along its length. The analyses were performed without special preparation of the surfaces.

Figure 6 – Stereo micrographies of tracks 1 to 4 along the surface of the convergent. (a) Tracks 1 and 2: C_{11} to C_{14} and C_{21} to C_{24}; e (b) Tracks 3 and 4: C_{31} to C_{34} and C_{41} to C_{44}.

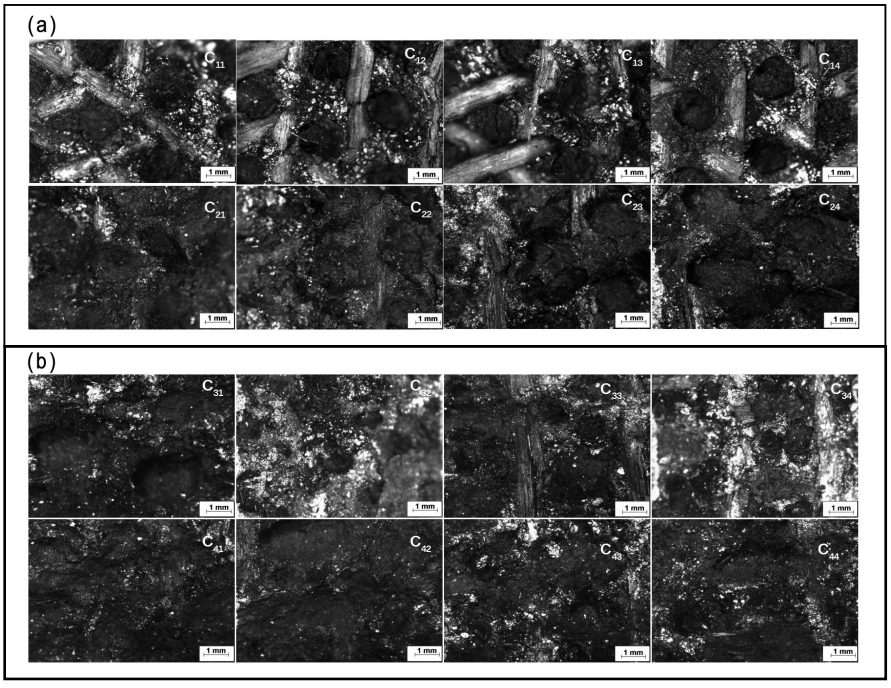

Source: The author.

3 RESULTS E DISCUSSION

3.1 Stereomicroscopy of the convergent of the tubing insert

Figure 6 presents a sequence of images obtained in the stereomicroscope with 16x magnification of the surface of the CRFC material of the convergent. The images were captured following the direction of the gas flow output.

It is observed in the tracks C11 to C14 and C21 to C24 strong erosion forming irregularities in the surface attacked by the flow of gases from the burning of the propellant, which shows the surface of the partially exposed fibers. This flow causes wear of matrix regions and rods (fibers). There are also regions that present light grey aspect, which were thermally affected by the flow of heated gases and correspond to a combustion residue of the propellant material. In the regions between C31 to C34 and C41 to C44, a more marked erosion is perceived in the carbon fiber reinforcement rods, especially those perpendicular to the gas flow. There is also an increase in erosion in the area of light gray regions.

Figure 7 shows that wear in rod regions and matrix regions was uniform, with less erosive effect. In addition, there is a greater presence of light gray regions, corresponding to residues from the combustion of the propellant material.

3.2 Stereomicroscopy of the throat of the tubing insert

In the throat region, shown in Figure 8, due to the higher passing speed of the gases, the wear mechanism was different from that observed in the convergent region. This is characterized by a more intense wear on the carbon matrix, leaving the fibers exposed. Few regions in light gray are noted, associated with residues from the combustion of the propellant material.

3.3 Stereomicroscopy of the divergent of the tubing insert

Figure 9 shows that in regions D11 to D14 and D21 to D24, at the exit of the throat to the divergent there was simultaneous wear of rod (fiber) and carbon matrix regions, being relatively more pronounced than that observed in the throat region. However, in tracks 3 and 4: D31 to D34 and D41 to D44, there was a predominance of wear in the carbon matrix.

3.4 Stereomicroscopy of the throat in the position adjacent and away from the flow of gases

3.4.1 Position adjacent to the passage of the gas flow in the throat

Figure 7 – Stereo micrographies of tracks 5 to 8 along the surface of the convergent.(a) Tracks 5 and 6: C_{51} to C_{54} and C_{61} to C_{64}; and (b) Tracks 7 and 8: C_{71} to C_{74} and C_{81} to C_{84}.

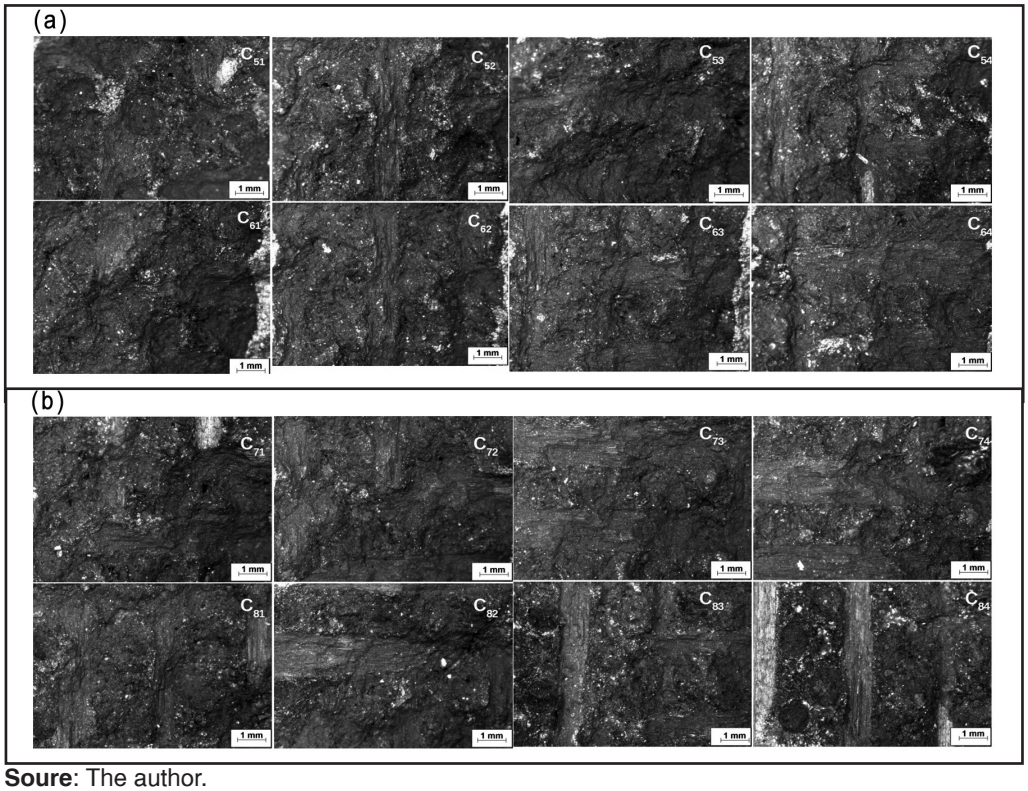

Soure: The author.

Figure 8 – Stereo Micrographies for tracks 1 to 4 along the throat's surface. (a) Tracks 1 and 2: T_{11} to T_{14} and T_{21} to T_{24}; and (b) Tracks 3 and 4: T_{31} to T_{34} and T_{41} to T_{44}.

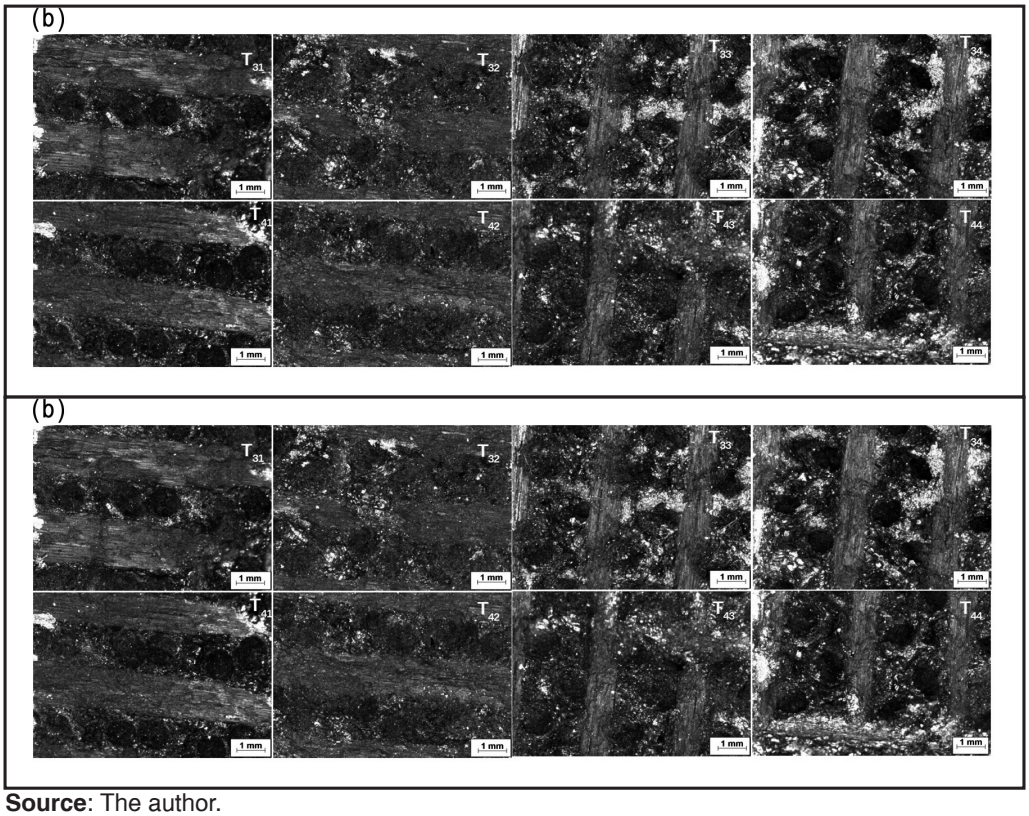

Source: The author.

Figure 9 – Stereo micrographies of tracks 1 to 4 along the surface of the divergent. (a) Tracks 1 and 2: D_{11} to D_{14} and D_{21} to D_{24}; and (b) Tracks 3 and 4: D_{31} to D_{34} and D_{41} to D_{44}.

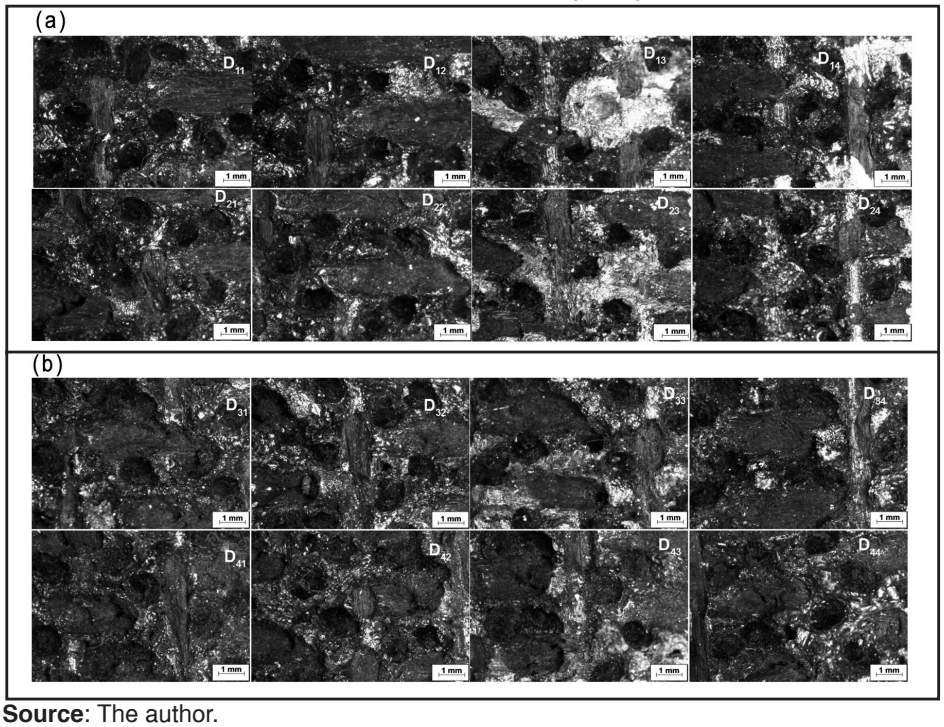

Source: The author.

Figure 10(a) shows the different composite constituents (fibers oriented at 90º and ±45º in relation to the plane of the image, matrix and pores), where an arrow indicates the direction of the gas flow. Figure 10(b) shows the magnification of the region highlighted in Figure 10(a), emphasizing the presence of a pore. Figures 10(c) to 10(f) show magnifications of Figure 10(b), highlighting the erosive wear on fibers at 90º [Figures 10(c) to 10(d)] and in fibers at ± 45º [Figure 10(c), Figures 10(e) and 10(f)]. In general, an erosion of the fibers occurred in all directions, forming irregularities in the surface attacked by gases, partially consuming the material and exposing its surface.

3.4.2 Position away from the flow of gases in the throat

Following images shown in Figure 11, aspects of multidirectional fibers are observed, the matrix formed by pyrolytic carbon deposits, obtained by the chemical infiltration technique in the gas phase (CVD/CVI) (1), fibers (2) and unfilled pores (3) in a region away from the gas flow.

Comparing the images in Figure 11 with those presented in Figure 10, it is clearly noted the absence of erosive and ablative effects on both the fibers and the matrix in the position away from the flow.

Figure 10 – Stereo micrographies obtained in a sample section embedded in the perpendicular direction and in a position adjacent to the flow of gases in the throat.

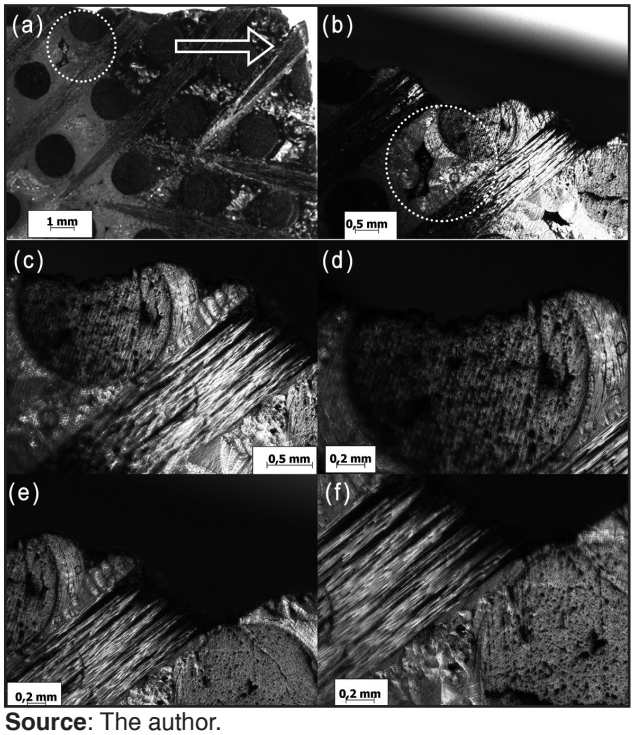

Source: The author.

Figure 11 – Stereo micrographies obtained in a sample section embedded in the perpendicular direction and in a position adjacent to the flow of gases in the throat.

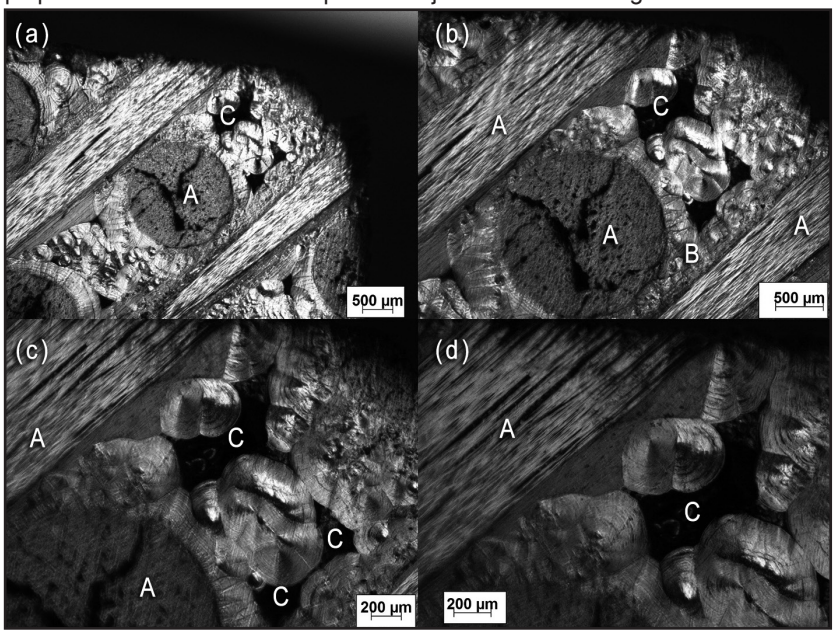

Source: The author.

3.5 Optical microscopy of the throat in the position adjacent and away from the flow of gases

3.5.1 Position adjacent to the flow of gases in the throat

Following images in Figure 12, aspects of reinforcement are observed (unidirectional rods) from the matrix formed by pyrolytic carbon deposits (1) and multidirectional fibers (2). It is evidenced in Figures 12(a) to Figure 12(d) the erosion of fibers, forming irregularities in the surface attacked by the gases, partially consuming the material and exposing its surface.

Figure 12 – Micrographies obtained in a sample section embedded in the perpendicular direction and in a position adjacent to the flow of gases in the throat.

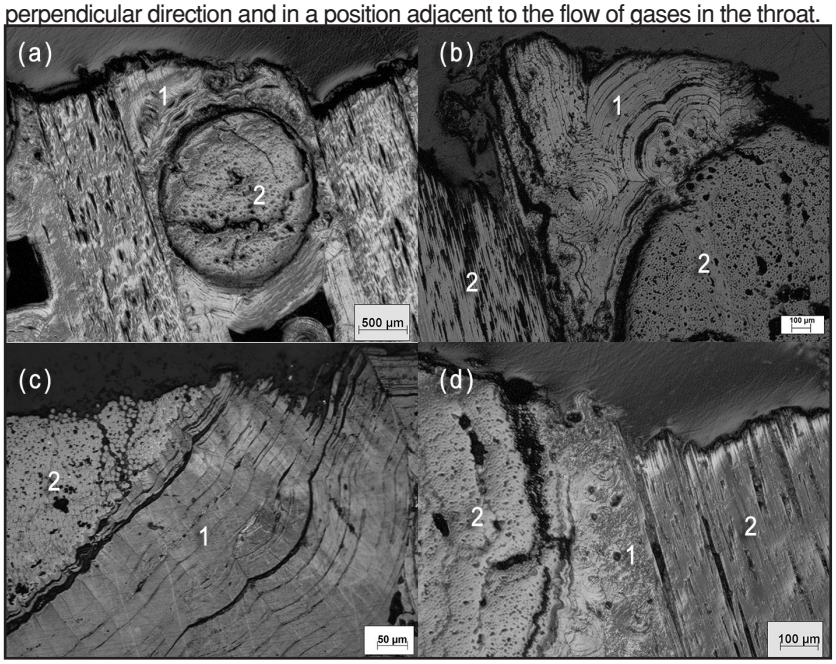

Source: The author.

3.5.2 Position away from the flow of gases in the throat

Following images in Figure 13, aspects of the matrix formed by pyrolytic carbon deposits (1) are clearly observed. Figure 13(c) shows the presence of longitudinally sectioned conical structures, specific to the carbon formation, and figure 13(d) shows the same conical structures, but transversally sectioned. Comparing the images in Figure 13 with those presented in Figure 12, it is clearly noted the absence of erosive and ablative effects on both the fibers and the matrix in the position away from the flow of gases from the burning of the propellant.

3.6 SEM of the throat's surface

The images in Figure 14 are similar to that presented by Levy Neto and Pardini, (2016, p. 212). Figure 14(a), indicated by the arrow, shows a region of confluence of pyrolytic carbon matrix, resulting from the densification process. In the central region of Figure 14(a) to figure 14(d) pyrolytic carbon lamellae are observed, obtained by the CVI/CVD process (1). The reinforcements (unidirectional rods) that make up the preform can also be identified (2) and, in Figure 14(a), it is perceived that they are oriented in different directions and involved by the carbon matrix.

Figure 13 – Micrographies obtained in a sample section embedded in the perpendicular direction and in a position away from the flow of gases in the throat.

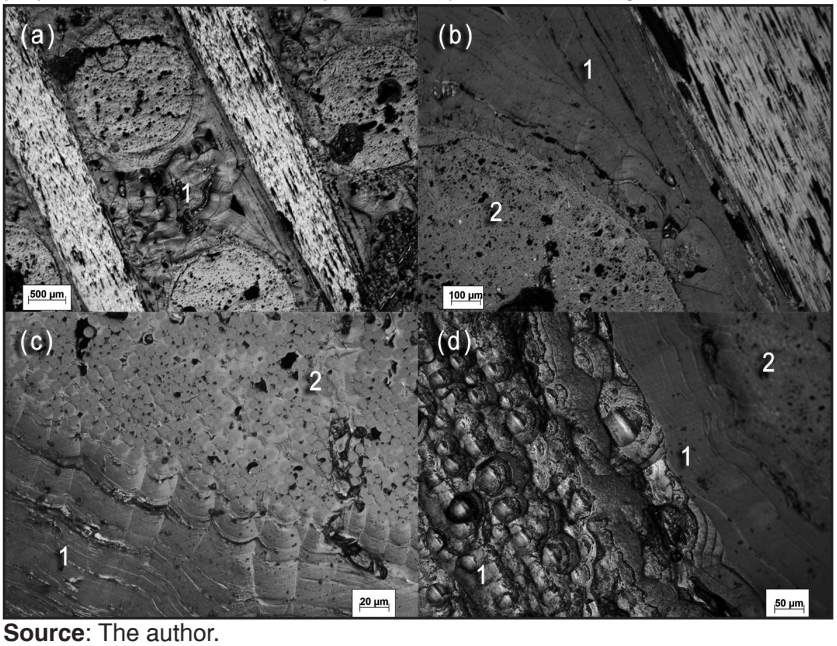

Source: The author.

Figure 14 – Images obtained by SEM in the parallel direction of the gas flow at different points of the throat surface.

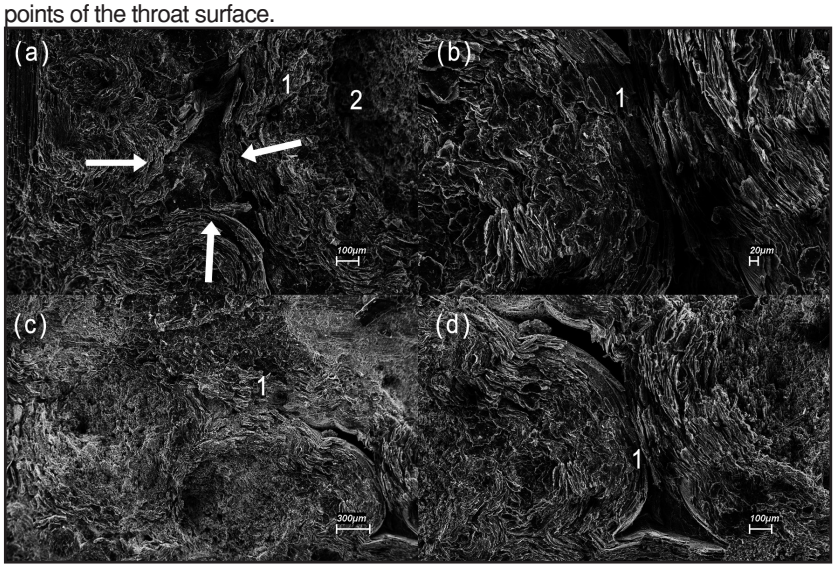

Soure: The author.

4 CONCLUSIONS

Regions near the throat section of a tubing insert were analyzed by microscopy techniques. Results of stereoscopy performed along points on the surface of an insert sample in the convergent, throat and divergent regions were presented. It was observed that the degradation mechanism of the material is changed according to the region analyzed. Wear is more pronounced in the convergent region when compared to the divergent region, although the velocity of passage of gases is lower in the convergent region, where the gas temperature is higher, and the angle of incidence of the flow of combustion gases on the material is also higher than in the divergent region.

The optical microscopy analysis performed in the throat section region showed that the erosion of the sample was more pronounced on the surface and that, in the regions farther away from the passage of the gas flow, no significant changes were observed.

The scanning electron microscopy, performed in the throat section, provided a more in-depth analysis of the morphology of the composite material, allowing to identify details of the reinforcing rods, consisting of carbon fiber filaments and, in the pyrolytic carbon matrix, where one can observe the different lamellae deposited by CVD/CVI.

The different analysis techniques used allowed to identify the erosion characteristics and systematize a procedure of analysis of the behavior of the material, in the face of the operating conditions, which can guide future work.

REFERENCES

AMERICAN SOCIETY FOR TESTING AND MATERIALS. **ASTM E3-11:** Standard guide for preparation of metallographic specimens. Pensilvânia. 2017.

GONÇALVES, A. **Caracterização de materiais termoestruturais a base de compósitos de Carbono Reforçados com Fibras de Carbono (CRFC) e carbonos modificados com Carbeto de Silício (SiC)**. 2008. Tese (Doutorado em Engenharia Mecânica e Aeronáutica) – Instituto Tecnológico de Aeronáutica, São José dos Campos, SP, 2008.

LEE, S. M. **Handbook of composite reinforcements**. Palo Alto: WILEY-VCH, 1993.

LEVY NETO, F.; PARDINI, L. C. **Compósitos estruturais**: ciência e tecnologia. 2. ed. São Paulo: Blucher, 2016. 418p.

LI, W.; HUANG, H.; XU, X. A coupled thermal/fluid/chemical/ablation method on surface ablation of charring composites, **Int. J. Heat Mass Transf**., v. 109, p. 725-736, 2017.

PARDINI, L. C.; GONÇALVES, A.; VIEIRA, S. D. Preformas multi-direcionais para compósitos termoestruturais. *In*: CONGRESSO BRASILEIRO DE ENGENHARIA E CIÊNCIA DOS MATERIAIS, 15., 2002, Natal. **Anais** [...]. Natal: CBCIMAT, 2002. p. 2161-2167.

RIBEIRO, J. L. P. **Predição de propriedades elásticas de compósitos termo estruturais com reforço multidirecional. 2006**. Dissertação (Mestrado em Engenharia Mecânica e Aeronáutica) – Instituto Tecnológico de Aeronáutica, São José dos Campos/SP, 2006. Disponível em: http://www.bdita.bibl.ita.br/tesesdigitais/lista_resumo.php?num_tese=62825. Acesso em: 6 jul. 2018.

RIBEIRO, J. L. P.; GREGORI, M. L.; PARDINI, L. C. Predição das propriedades elásticas de compósitos termoestruturais com reforço multidirecional. **Matéria**, Rio de Janeiro, v. 13, n. 1, jan./mar. 2008.

RICCIO, A. *et al*. Optimum design of ablative thermal protection systems for atmospheric entry vehiclese. **Appl. Therm. Eng**., v. 119, p. 541-552, 2017.

SILVA, R. J. **Plasma térmico para ablação de materiais utilizados como escudo de proteção térmica em sistemas aeroespaciais**. Dissertação (Mestrado em Engenharia Mecânica e Aeronáutica) – Instituto Tecnológico de Aeronáutica, São José dos Campos, 2011. Disponível em: http://www.bdit.bibl.ita.br/tesesdigitais/lista_resumo.php?num_tese=62019. Acesso em: 6 jul. 2018.

SILVA, W. G. **Qualificação de materiais utilizados em sistemas de proteção térmica para veículos espaciais**. Tese (Mestrado em Física dos Plasmas) - Instituto Tecnológico de Aeronáutica , São Jose dos Campos, 2009.

SUTTON, G. W. The initial development of ablation heat protection: an historical perspective, **Sp. Chron.**, v. 59, p. 16-28, 2006.